Journal Pre-proofs

The energy approach to fatigue crack growth of S355 steel welded specimens subjected to bending

Dariusz Rozumek, Janusz Lewandowski, Grzegorz Lesiuk, Zbigniew Marciniak, José A. Correia, Wojciech Macek

PII: S0167-8442(22)00216-6
DOI: https://doi.org/10.1016/j.tafmec.2022.103470
Reference: TAFMEC 103470

To appear in: *Theoretical and Applied Fracture Mechanics*

Received Date: 1 April 2022
Revised Date: 16 June 2022
Accepted Date: 27 June 2022

Please cite this article as: D. Rozumek, J. Lewandowski, G. Lesiuk, Z. Marciniak, J.A. Correia, W. Macek, The energy approach to fatigue crack growth of S355 steel welded specimens subjected to bending, *Theoretical and Applied Fracture Mechanics* (2022), doi: https://doi.org/10.1016/j.tafmec.2022.103470

The energy approach to fatigue crack growth of S355 steel welded specimens subjected to bending

Dariusz Rozumek[a,*], Janusz Lewandowski[a], Grzegorz Lesiuk[b], Zbigniew Marciniak[a], José A. Correia[c], Wojciech Macek[d]

[a]Department of Mechanics and Machine Design, Opole University of Technology, ul. Mikołajczyka 5, 45-271 Opole, Poland

[b]Department of Mechanics, Materials Science and Biomedical Engineering, Wrocław University of Science and Technology, Smoluchowskiego 25, 50-370 Wrocław, Poland

[c]INEGI/Faculty of Engineering, University of Porto, Rua Dr. Roberto Frias, 4200-465 Porto, Portugal

[d]Faculty of Mechanical Engineering and Ship Technology, Gdańsk University of Technology, Gabriela Narutowicza 11/12, 80-233 Gdańsk, Poland

ABSTRACT

The study presents the results of the research on the rate of fatigue crack growth subjected to bending in the ferritic-pearlitic structure. The studies were carried out at a constant amplitude of the moment and at various values of the load ratios R and at the operating frequency of the machine of 28.4 Hz. Flat specimens made of S355 steel and with fillet welds and with double-sided blunt external notches as well as concave and convex welds were tested. The tests were performed on specimens without and after relief annealing. The study showed that the heat

* Corresponding author. Tel.: +48-77-449-8410.
E-mail address: d.rozumek@po.edu.pl (D. Rozumek).

treatment had an influence on the dispersion of the test results described by the energy parameter. It was also observed that the effect of the applied treatment increased the rate of fatigue crack growth.

Keywords: Welds, FCGR, Heat treatment, J parameter

Nomenclature

a	- length of crack
h	- height of weld
r	- radius of the stress concentrator
t	- thickness of specimen
w	- width of weld
A_5	- percentage elongation after specimen breakage
da/dN	- rate of fatigue crack growth
E	- modulus of longitudinal elasticity
Fg	- loading force
K_t	- theoretical factor of the notch stress concentration
M	- bending moment
n'	- cyclic strain hardening exponent
N	- cycles number
R	- stress ratio
ΔJ	- J-integral parameter range
ΔK	- range of stress intensity factor
$\Delta\sigma$	- range of stress

ν - Poisson‘s ratio

σ_y - yield strength

σ_u - ultimate strength

Abbreviations

BEM - boundary element method

CTOD - displacement of the opening of the tip of the crack

FCGR - fatigue crack growth rate

HAZ - heat-affected zone

HT - heat treatment

SIF - stress intensity factor

TIG - tungsten inert gas

Subscripts

a - amplitude

I - mode one

1. Introduction

One of the main goals in the design structure process is the efficient use of material properties. Such a structure must meet the safety conditions in accordance with the standards. One of the main factors taken into account when designing is, apart from safety, the economy. The role of scientists is to carry out research and focus on the durability and susceptibility to the development of fatigue cracks in the structure. Which will contribute to the fact that the structures are more durable and work in failure-free conditions for a long period of time [1,2]. Many structures are joined by welding methods that are durable and relatively cheap. Welding, as a method of inseparable joining of elements, is widely used in various branches of the

industry [3]. For this reason, this topic is of interest to many scientists, and the results of the research are presented in journals around the world [4,5]. However, due to the constantly growing need to improve the quality of welded constructions, and thus increase their safety and durability, it is still very desirable [6]. The current science focuses on creating such welded joints that effect the durability and reliability of these joints [7,8].

The idea of employing energy-based approaches to material fatigue started from the pioneering research of Prof. Lazzarin [9,10] and is still very interesting for scientists which are reflected in new approaches [11].

The paper shows how different shapes of welds, load and heat treatment influence the fatigue life in the energy approach. The presented research and analyzes may be useful in the design of welded joints and the influence of various factors on the joint.

The work [7] also investigated the effect of various types of welds and related imperfections on the growth of fatigue cracks (using SIF for description) under tension and torsion.

In the study [12], the welded elements which were damaged during cyclic loads were analyzed. During the tests, it was found that the type of material, the type of notch and the load amplitude are the factors influencing the cyclical lifetime of the tested welded elements.

In ref. [13], the influence of the cyclic load on the redistribution of residual stresses in the area of the joint face of the butt-welded was investigated with the use of numerical simulations.

In ref. [14] for welded joints, a local approach was used to predict the cyclical life of sharp notched elements. The research is based on analytical expressions of the local stress field and presents a simplified form that is oriented towards practical application.

The goal of the study is to show the research results on the rate of FCG used for welded components of the tested material without and after relief annealing, subjected to bending for various stress ratios R, in terms of energy described by the J-integral parameter.

2. Research procedure

2.1. Material and its properties

The material of this study is the S355 structural steel [15]. The geometries of the specimens for testing the fatigue crack growth were characterized by symmetrical side concave and convex welds and are presented in Fig. 1. The samples were made of two parts joined together by fillet welds from a drawn rod of diameter 30 mm [5]. The specimen surface was made by milling, and in the next step polished with sandpaper of various grit.

Figure 1.

The chemical mixture and static properties of S355 steel are shown in tables 1 and 2. The research was done at the Opole University of Technology.

Table 1.

Table 2.

Welded joints were obtained by the TIG method with the use of an argon shield. W-42-2-W2Sil welding wire was used in the welding process in accordance with EN ISO 636 [16]. All samples were previously checked by non-destructive testing [17]. Non-destructive tests were aimed at eliminating specimens with defects (discontinuities), that could affect the test results. The studies on the development of ruptures was performed on solid specimens and two types of welded specimens (concave and convex welds) without HT and after application relief annealing. Relief annealing was performed at a temperature of 630˚C for 2 hours.

The welded joints in the specimens were made manually according to Figure 1 (global geometry of specimens). During the tests, differences in the local geometries of individual samples were observed. The specimens with the largest geometry differences were rejected. Slight differences occurred mainly in the radii at the weld toe ρ. In specimens with concave welds, the ρ radii were within the range of 2.0 ÷ 2.5 mm. In specimens with convex welds, the values of the radius at the bottom of the notch ρ ranged from 0.2 to 0.28 mm. The leg length of the welds L for all welded specimens was within the range of 2.6 ÷ 2.75 mm. The weld inclination angle β for concave welds ranged from 168 to 174°, and for convex welds it was much smaller and ranged from 108 to 122°. The determination of the local geometry for the tested specimens is shown in Figure 2.

Figure 2.

The OLYMPUS IX70 optical microscope was used for metallographic studies using polarized light. Figure 3 shows the joint structures without and after heat treatment.

Figure 3.

The Vickers method was used to test the hardness. The microhardness was checked on a LECO MH200 device with a loading of 0.98 N. The time of loading application used in the hardness tests was approximately 3 s. The tests were performed based on the EN ISO 9015-1 standard [18].

2.2. Fatigue test

The fatigue crack growth rate was tested on the setup of fatigue machine MZGS – 100 shown in Figure 4 [19, 20]. During the tests, the bending moment amplitude was controlled (load with a controlled force) with a sinusoidal waveform and works under loading frequency of 28.4 Hz. The theoretical factor of notch operation, K_t, in the solid sample with concave and convex welds subjected bending was computed according to model [21] and equals to 1.38 and 1.56, respectively. The specimens fixed on one side were tested at the constant stress ratios R = - 1, 0, and the moment amplitude, M_a = 9.2 N·m. The value of this moment after conversion gives the stresses of σ_a = 383 and 766 MPa (for a solid sample). Bending was carried out on a lever, the length of which was 0.2 m. The increase in fatigue cracks was visually seen on the sample area (light microscope - 20x magnification) and measured with an mounted micrometer. The fatigue life of N was regularly recorded. The measurement results are presented in the form of graphs of the length of crack as a function of the cycles number N, as well as the diagrams of the rate of growth of fatigue cracks as a function of the ΔJ_I parameter range.

Figure 4.

3. Results and discussion

In carrying out the fatigue investigations, the initiation and growth of fatigue cracks in the welded areas was observed. The crack development was most often observed unilaterally in the specimen. Figure 3 shows the joint structures without and after heat treatment. The welded structure (with both concave and convex welds) without heat treatment is shown in Fig. 3a, which shows the shape of the dendrites and has the Widmanstatten structure. The material structures of the samples changed after subjecting them to heat treatment (HT). After applying

HT, where the material of the welded sample after annealing, it was characterized by the grains of bainite and sorbitol observed in the HAZ and the welds. This structure is shown in Figure 3b. The base material consisted of fine and very fine grains of ferrite and perlite, respectively, and was streaked.

Fig. 5 shows the averaged values for two types of welds (concave and convex welds had similar hardness in individual zones) and three zones occurring in the joint, such as starting metal, heat affected zone (HAZ) and weld.

Figure 5.

The microhardness in welds before and after heat treatment was measured and it was found that after annealing, the hardness of welded joints decreased significantly. The microhardness of welds with non-applied HT changed from the lowest for the base material to the highest in the HAZ, while after heat treatment the microhardness was less fluctuating than without HT [4]. In the case of a joint without HT, the highest microhardness was recorded in HAZ, and the lowest for the parent material, but they were higher than the microhardness after HT. The shape of the weld had little effect here. Before HT, the microhardness ranged from 188–274 $HV_{0.1}$, and after heat treatment it was 125–154 $HV_{0.1}$. The hardness of the fundamental metal for the tested specimens is very similar. In addition, hardness changes were observed due to the influence of carbon or the lack of it in the martensite layers. The greatest hardness is noted in fusing into the HAZ. The confirmation of the greatest hardness for HAZ in the area of fusion is given in [22]. Whereas, looking in the direction the weld metal, the hardness decrease.

When carrying out the tests, the propagation on one side of the specimen was first observed, and after the period of the cycles number, the propagation of the rupture on the other side of the specimen was also noticed.

Fig. 6 shows the FCG in relation to its durability for specimens without heat treatment and R = -1, 0, and Fig. 7 presents the results for samples after relief annealing and the same stress ratios. As shown in Figs. 6 and 7 the greatest durability has samples made of fundamental metal for R = -1 and 0, as well as applied or not heat treatment. Then the fatigue life of S355 steel decreases for concave and convex welded specimens. Since convex welded specimens have sharp notches, initiation and propagation are the fastest in them. After applying the HT, we can see that the order of the crack growth in the welded specimens is preserved. There are noticeable differences in the durability of solid and welded samples without and after HT for R = - 1 and 0. The hardness of the specimens in different zones has an influence on the different durability. The lowest hardness is for a solid specimen, which is 189 $HV_{0.1}$ without HT, and 127 $HV_{0.1}$ after HT. On the other hand, the hardness of the sample with welds without HT ranged from 197 to 284 $HV_{0.1}$, and after heat treatment it is in the range of 132-142 $HV_{0.1}$. The hardness of the specimens influences the FCGR, and this, in turn, also affects the obtained experimental coefficients (C, m).

Figure 6.

Figure 7.

Due to the fact that from the beginning of the crack measurements, the stresses are greater than the yield strength and increase as the rupture develops, the energy approach with the range of

parameter ΔJ was used for the calculation of changes in stresses and strains. The investigation results for the FCGR (shown in Figs. 8, 9) were described by the relationship [23]

$$\frac{da}{dN} = C(\Delta J_I)^m \tag{1}$$

where C, m – constants in research from equation (1).

The energy parameter ΔJ_I was computed from [24]

$$\Delta J_I = \Delta K_I^2 / E + \pi Y^2 M_k a\left(\Delta\sigma\Delta\varepsilon_p / \sqrt{n'}\right) \tag{2}$$

where $M_k = C \cdot \left(\frac{a}{t}\right)^k$ - the coefficient that includes the structural notch, i.e. the shape and size of the weld in the welded joint [25], while the coefficients B, k and Y are given in [5], $\Delta\varepsilon_p$ - plastic deformation at the rupture tip.

In the calculation of the SIF and J parameters in the samples, a numerical approach was used with the using of Franc3D software [26]. The computations were made using BEM, introducing a nonlinear model of material. Stress, CTOD and SIF computations were made for the 3-dimensional geometric models of the samples. The triangular boundary elements were employed to reflect the geometry of specimens(the solid specimen had 1,580 elements, 1,085 the sample for concave joint and 1,810 for convex joint). During numerical computations, the points of crack initiation corresponding to the crack initiation in the research for similar loads and directions of rupture development were modeled. The calculated stresses, strains and SIF parameters made it possible to determine the J parameter from the equation (2).

The models of samples used for numerical calculations were made in the ABAQUS software, from which the results in the form of maps of stresses and strains were obtained. The

FRANC3D software was used to numerically generate crack growth paths. The crack initiated in the course of modeling is subjected to numerical analysis, as a result of which the program calculates changes of stresses on the front of the crack. Then, it calculates the SIF and on this basis determines the specific values of the crack growth path. The FRANC3D software performs calculations of the FCGR, most often based on the stress fracture model, e.g. using the Paris equation. Numerical analyses were performed in the elastic-plastic range. The finite element meshes in numerical models were built from tetrahedra. In the samples with concave welds, the initial number of elements was 308,026, and in the samples with convex welds, it was 302,092. In each of the samples, the highest density and smallest size of finite elements were modeled in the area with the highest concentration of stresses and cracks. The smallest size of the finite element was 0.02 mm. Figure 10 shows a diagram of the modeled restraint and loading of samples with a pair of forces.

Figures 8 and 9 show the experimental results of the FCGR against the ΔJ. The graphs in Fig. 8a for stress ratio R = -1, we can observe that in the initial crack period of the solid specimen, the rate of FCG is $da/dN = 1.00 \cdot 10^{-7}$ m/cycle, the velocity increases, and before the sample is damaged, the value is $da/dN = 1.85 \cdot 10^{-7}$ m/cycle [7]. Welded specimens (Fig. 8a), the velocities at the beginning are similar and for samples with concave welds they are $da/dN = 1.33 \cdot 10^{-7}$ m/cycle and for convex joints specimens, the velocity is $da/dN = 1.20 \cdot 10^{-7}$ m/cycle. Then, for convex joints samples, the rate of crack development increases to a value of $da/dN = 5.20 \cdot 10^{-7}$ m/cycle, and for samples with concave joints, the rates of crack development reach a value of $da/dN = 4.13 \cdot 10^{-7}$ m/cycle. In fig. 8b for R = -1 we can see a very good correlation of the test results for all samples (both solid and welded) with the calculated results, which causes the effect of heat treatment. The results of tests and computations for the three types of specimens coincide. A similar, but slightly worse correlation of the test results is observed in Fig. 9b for

R = 0. This behavior of steel is caused by the residual stress in the welds (the values reached a maximum of 280 MPa [17]) and the lack of homogeneity of the structure in the tested samples in which HT was not used. In both full and welded samples for two R = -1 and 0 (Figs. 8a, 9a) without relief annealing, a greater scatter of results is observed than for samples after heat treatment. In all cases of the tested specimens relief annealing was applied, a clear increase in the propagation velocity was observed. With the use of heat treatment, the slope of the lgda/dN - lgΔJ curves becomes steeper for both R = - 1 and 0. Comparing the results in Figs. 8 and 9 for R = - 1 and 0, it can be noticed for R = 0 a clear increase in the value of ΔJ_I both for specimens without and after heat treatment. A shift of the cracking curves 1, 2, 3 is observed from $\Delta J_I = 1.00 \cdot 10^{-2}$ MPa·m to $\Delta J_I = 1.00 \cdot 10^{-1}$ MPa·m. In Fig. 8, for the same range of $\Delta J_I = 1.00 \cdot 10^{-2}$ MPa·m, an increase in the FCGR can be observed for the sample with concave and convex joints compared to a solid specimen. We observe a similar behavior also for R = 0 (Fig. 9).

The durability of the solid specimens is in all cases the highest. The durability of specimens with concave joints is little lower than that of solid specimens, but higher than those of specimens with convex joints, because a sharp concentrator stresses weakens the convex joints and makes them the least durable.

Figure 8.

Figure 9.

Figure 10.

Fatigue cracks initiated symmetrically in both types of welded specimens, as visualized in the macro-images shown in Figures 11a and 11b. The fractograms shown in Figure 11 demonstrate the dominance of the fatigue fracture mechanism. However, due to the significant contact areas

of the fractured specimens, significant slip and crush zones resulting from the mutual contact of the specimens were also visualized. This is particularly evident for the concave type specimen in the zone marked by the box - Fig. 11a - on the bottom of the specimen. Similar areas, were observed in smaller proportion in convex - Fig. 11b specimens, where the dominant fatigue mechanism at crack initiation was apparent. Stable crack growth was observed up to 2,5-3 mm in case of the concave welds – Fig. 11c. The areas of stable propagation for the convex weld are shown in Figure 11d. Analyzes were made for a rupture of approximately 1.11 mm and a propagation rate estimated to be $1\text{-}2 \cdot 10^{-7}$ m/cycle. In this area, a typical transcrystalline crack growth mechanism was observed through ferrite and pearlite grains with small shear areas (flat surfaces). The possible mechanism of the formation of shear regions is due to the residual compressive stresses arising during welding, and focusing in the area of the rupture tip in the tested types of joints.

Figure 11.

The coefficients C, r and the exponent m used in the equation (1) were obtained from the results of research using the least squares method and are shown in Table 3. In all cases, except for Fig. 8a, curve 2, we can see large values of the coefficients of correlation r.

Table 3.

4. Conclusions

The research results on the rate of FCG in cyclic bending revealed that:

1. It has been shown that the geometry of the weld face (convex or concave) significantly affects the durability of the entire joint.

2. Stress relief annealing reduces the variation in hardness of the HAZ and the welded joints with respect to the hardness measurement of samples in which the heat treatment process was not applied.
3. It was found that the samples in which HT was applied had a higher rate of crack development compared to the samples where HT was not applied for both R = -1 and 0.
4. It was noticed that in the samples after HT there were a smaller scatter of the results of the rate of FCG described by the ΔJ parameter than in the samples where HT was not used.

References

[1] Marshall PW. Design of welded tubular connections. Basis and use of AWS code provisions. Elsevier, 1992

[2] Carpinteri A., Ronchei C., Scorza D., Vantadori S. Fracture mechanics based approach to fatigue analysis of welded joints, Eng. Failure Analysis 49 (2015), pp. 67-78, 10.1016/j.engfailanal.2014.12.021

[3] Kawiak M., Balitskii A. Embrittlement of welded joints of tram rails in city environments. Eng. Fail. Anal., 85 (2018), pp. 97–103, 10.1016/j.engfailanal.2017.12.011

[4] Zhi-Gang Xiao, Tao Chen, Xiao-Ling Zhao, Fatigue strength evaluation of transverse fillet welded joints subjected to bending loads. Int. J. Fatigue, 38 (2012), pp. 57–64, 10.1016/j.ijfatigue.2011.11.013

[5] Rozumek D., Lewandowski J., Lesiuk G., Correia J. The influence of heat treatment on the behavior of fatigue crack growth in welded joints made of S355 under bending loading. Int. J. Fatigue, 131 (2020), 10.1016/j.ijfatigue.2019.105328

[6] Nejad RM., Sina N., Moghadam DG., Branco R., Macek W., Berto F. Artificial neural network based fatigue life assessment of friction stir welding AA2024-T351 aluminum alloy and multi-objective optimization of welding parameters. Int. J. Fatigue, 160 (2022), 106840, 10.1016/j.ijfatigue.2022.106840

[7] Wahab M.A., Alam M.S. The significance of weld imperfections and surface peening on fatigue crack propagation life of butt-welded joints. J. of Materials Processing Technology, 153–154 (2004), pp. 931–937, 10.1016/j.jmatprotec.2004.04.150

[8] Tanaka S., Kawahara T., Okada H. Study on crack propagation simulation of surface crack in welded joint structure. Marine Structures, 39 (2014), pp. 315-334, 10.1016/j.marstruc.2014.08.001

[9] Lazzarin, P., Livieri P., Berto F., Zappalorto M. Local strain energy density and fatigue strength of welded joints under uniaxial and multiaxial loading. Eng. Fract. Mech., 75 (2008), pp. 1875-1889, 10.1016/j.engfracmech.2006.10.019

[10] Lazzarin P., Berto F., Gómez F.J., Zappalorto M. Some advantages derived from the use of the strain energy density over a control volume in fatigue strength assessments of welded joints, Int. J. Fatigue, 30 (2008), pp. 1345-1357, 10.1016/j.ijfatigue.2007.10.012

[11] Kujawski D. A damaging function ΔK_d for analyzing FCG and R-ratios in metallic materials. Theoretical and Applied Fracture Mechanics, 116 (2021), 10.1016/j.tafmec.2021.103091

[12] Pakandam F., Varvani-Farahani A. A comparative study on fatigue damage assessment of welded joints under uniaxial loading based on energy methods. Proc. Eng., 2 (2010), pp. 2027–2035, 10.1016/j.proeng.2010.03.218

[13] Ferro P., Berto F., James M.N. Asymptotic residual stresses in butt-welded joints under fatigue loading. Theoretical and Applied Fracture Mechanics, 83 (2016), pp. 114-124, 10.1016/j.tafmec.2016.02.002

[14] Atzori B., Meneghetti G., Susmel L. Estimation of the fatigue strength of light alloy welds by an equivalent notch stress analysis. Int J Fatigue, 24 (2002), pp. 591-599, 10.1016/S0142-1123(01)00113-X

[15] Macek W., Marciniak Z., Branco R., Rozumek D., Królczyk G.M. A fractographic study exploring the fracture surface topography of S355J2 steel after pseudo-random bending-torsion fatigue tests, Measurement 178 (2021), 10.1016/j.measurement.2021.109443

[16] EN ISO 636. Welding consumables. Rods, wires and deposits for tungsten inert gas welding of non-alloy and fine-grain steels, 2008

[17] Lewandowski J., Rozumek D. Fatigue crack growth in welded S355 samples subjected to bending loading, Metals 11, (2021), Article 1394, 10.3390/met11091394

[18] EN ISO 9015-1. Destructive Tests on Welds in Metallic Materials - Hardness Testing - Part 1: Hardness Test on arc Welded Joints Defines, 2011

[19] Rozumek D., Macha E. Elastic-plastic fatigue crack growth in 18G2A steel under proportional bending with torsion loading, Fatigue Fract. Eng. Mater. Struct. 29 (2006), pp. 135-145, 10.1111/j.1460-2695.2006.00972.x

[20] Macek W., Rozumek D., Królczyk G.M. Surface topography analysis based on fatigue fractures obtained with bending of the 2017A-T4 alloy, Measurement 152 (2020), 10.1016/j.measurement.2019.107347

[21] Thum A., Petersen C., Swenson O. Verformung, Spannung und Kerbwirkung. VDI, Duesseldorf, 1960

[22] Yi-Bo Shang, Hui-Ji Shi, Zhao-Xi Wang, Guo-Dong Zhang, In-situ SEM study of short fatigue crack propagation behavior in a dissimilar metal welded joint of nuclear power plant, Materials & Design 88 (2015), pp. 598-609, 10.1016/j.matdes.2015.08.090

[23] Dowling N.E., Begley J.A. Fatigue crack growth during gross plasticity and the J-integral, In Mechanics of Crack Growth, ASTM STP 590 (1976), pp. 82-103

[24] Rozumek D. Influence of the slot inclination angle in FeP04 steel on fatigue crack growth under tension, Materials & Design 30 (2009), pp. 1859-1865, 10.1016/j.matdes.2008.09.017

[25] Hobbacher A. IIW Recommendations for fatigue design of welded joints and components, WRC Bulletin 520, Welding Research Council, New York, 2009, pp. 144

[26] www.cfg.cornell.edu/software.html

Figure 1

a)

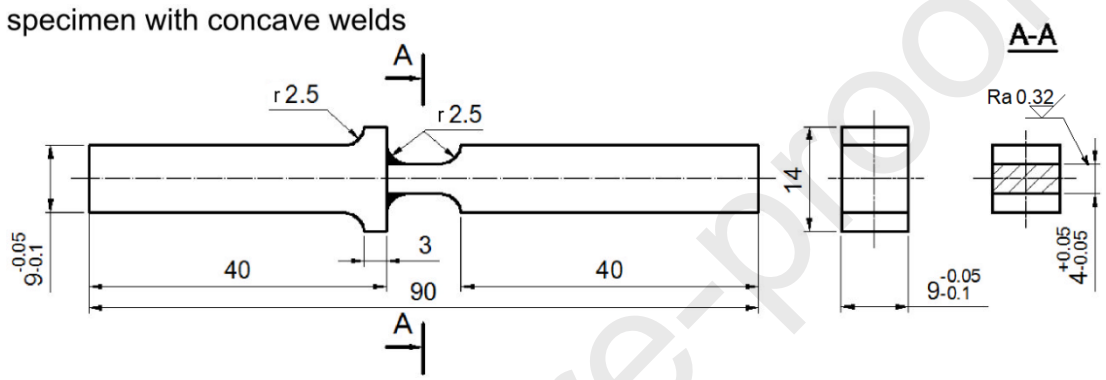

b)

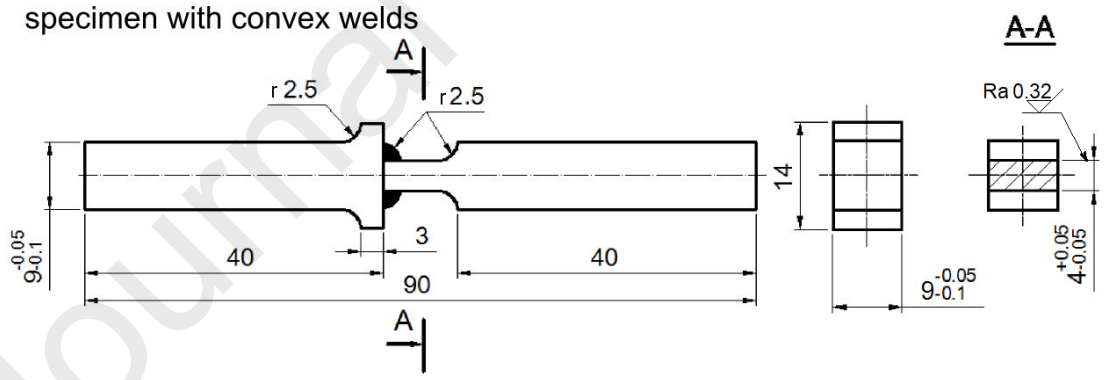

Figure 2

a)

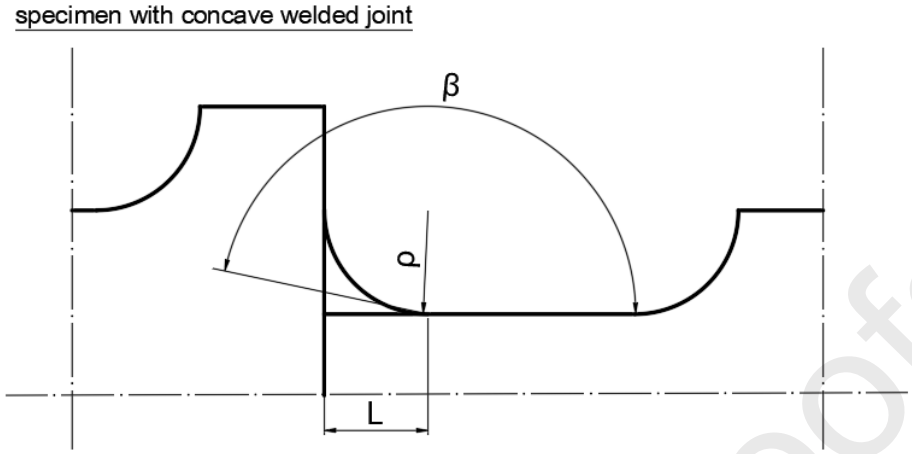

b)

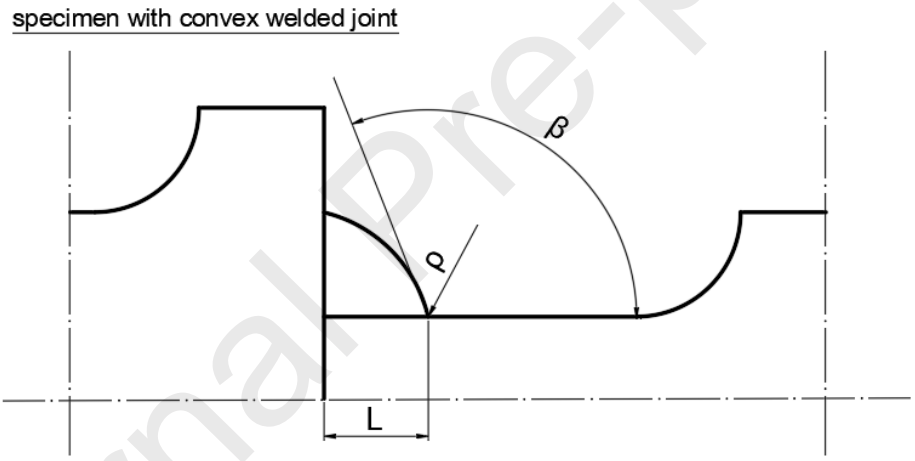

Figure 3

a)

b)

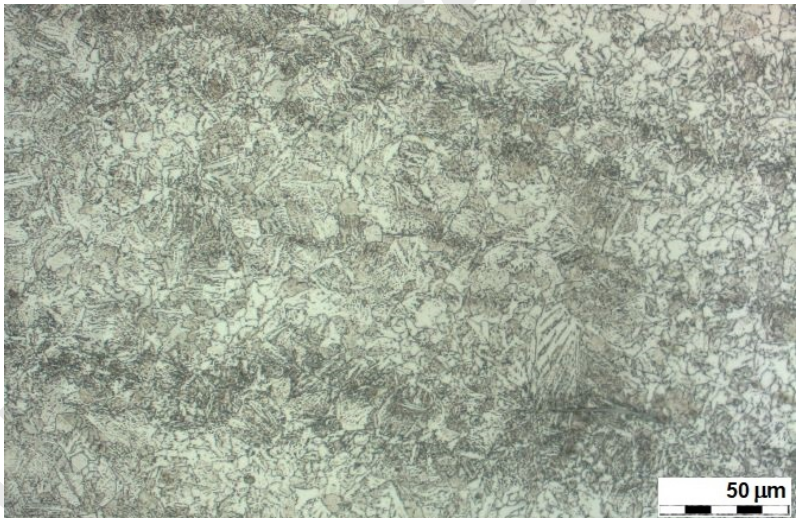

Figure 4

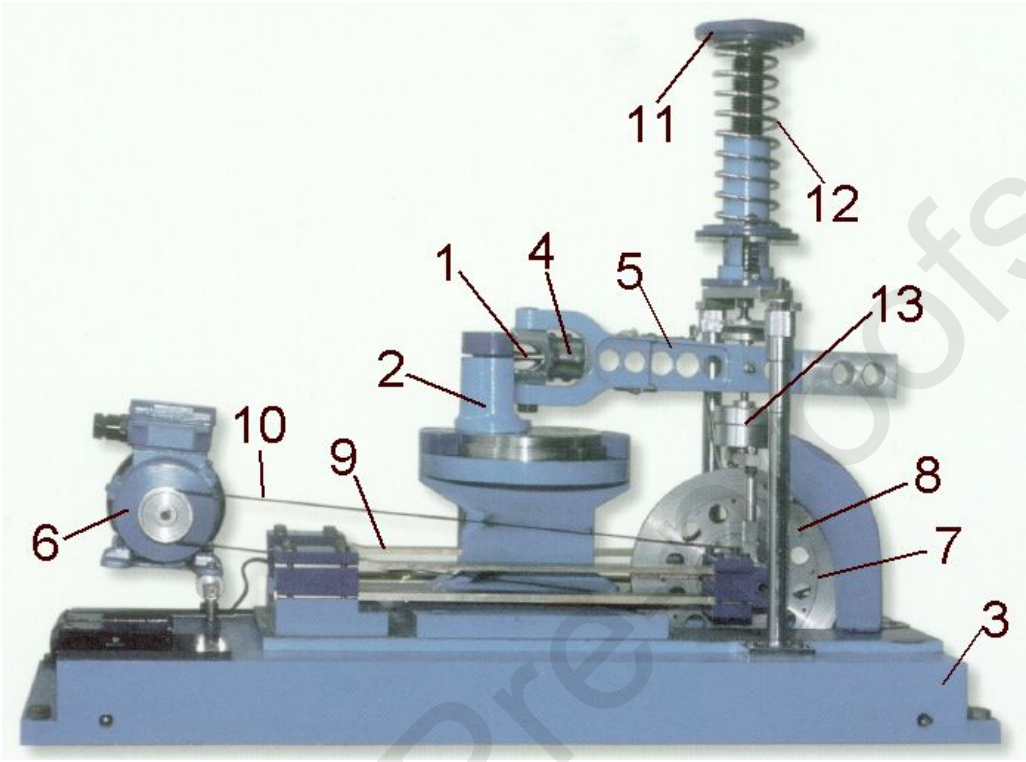

Figure 5

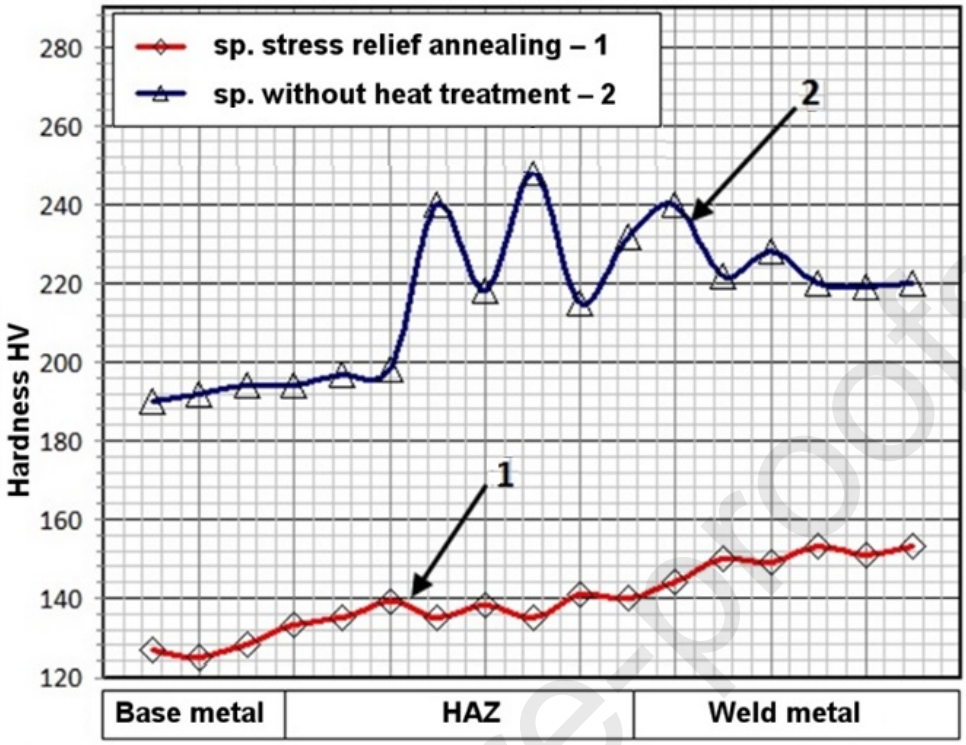

Figure 6

a)

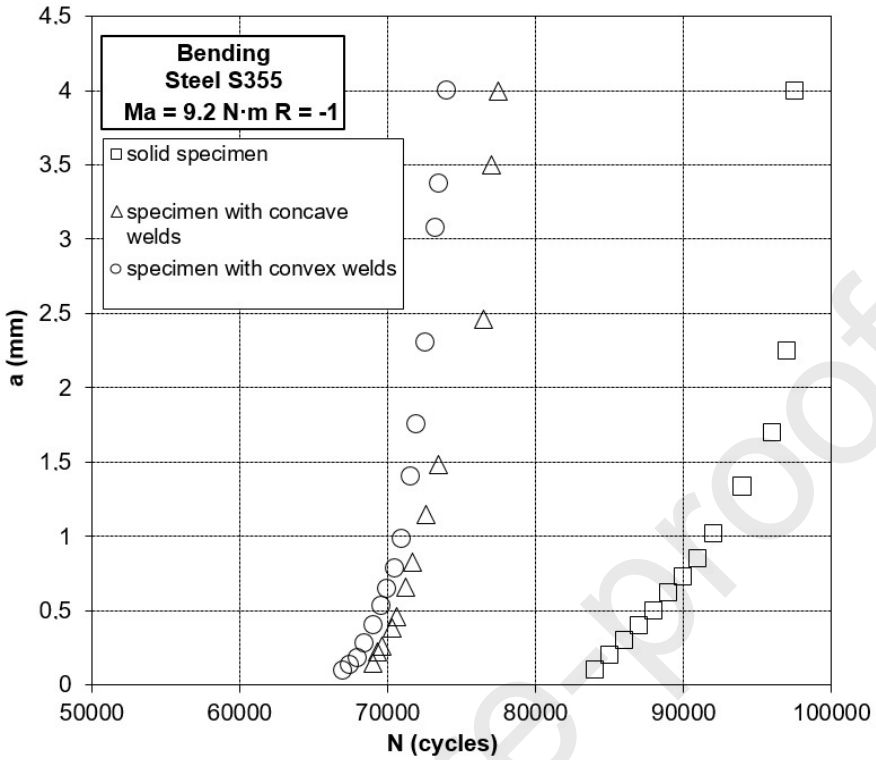

b)

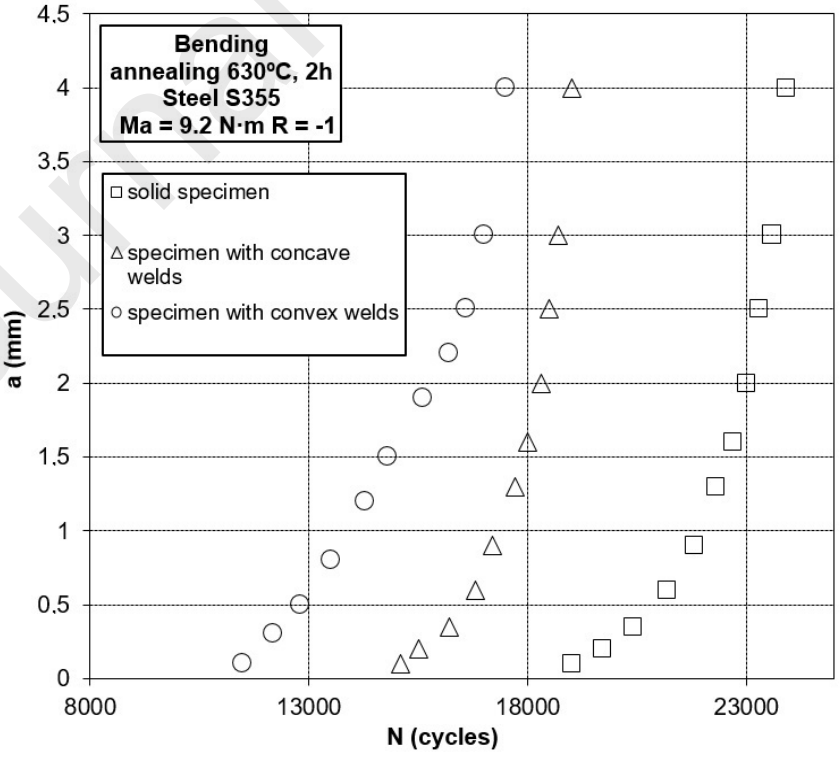

Figure 7

a)

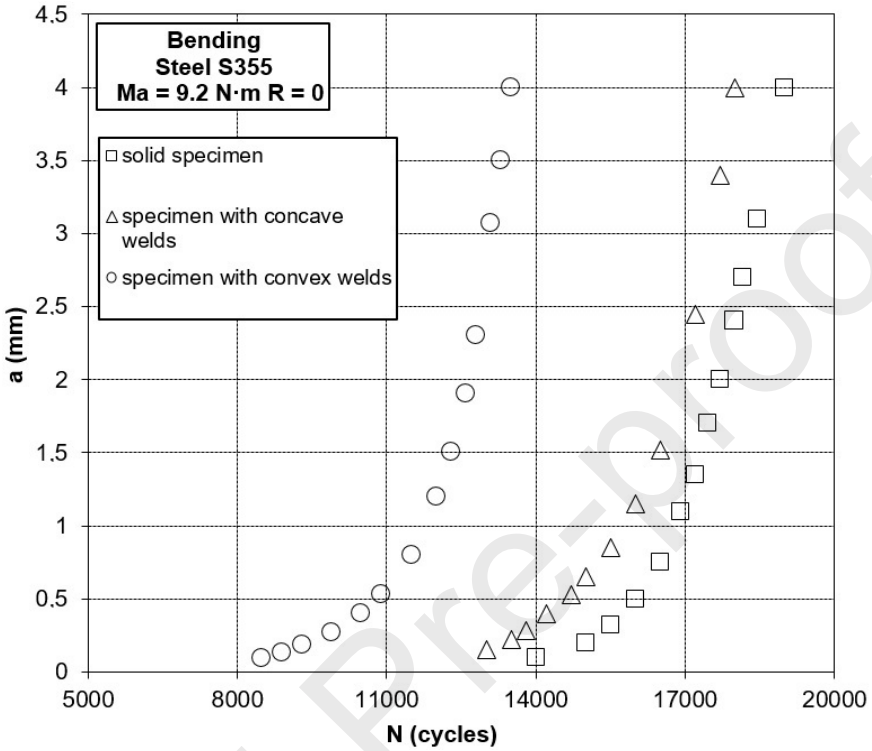

b)

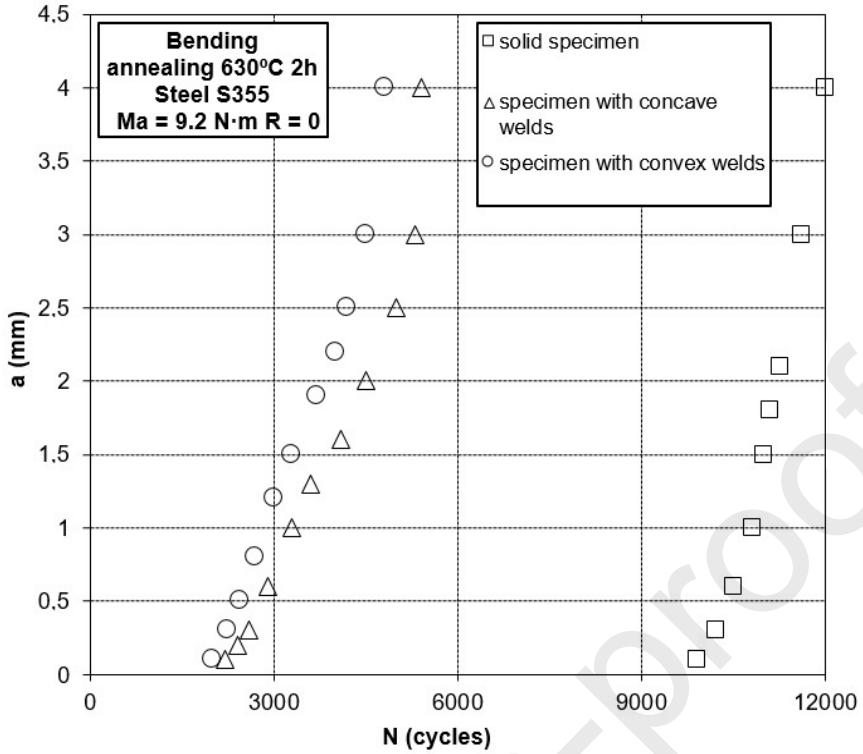

Figure 8

a)

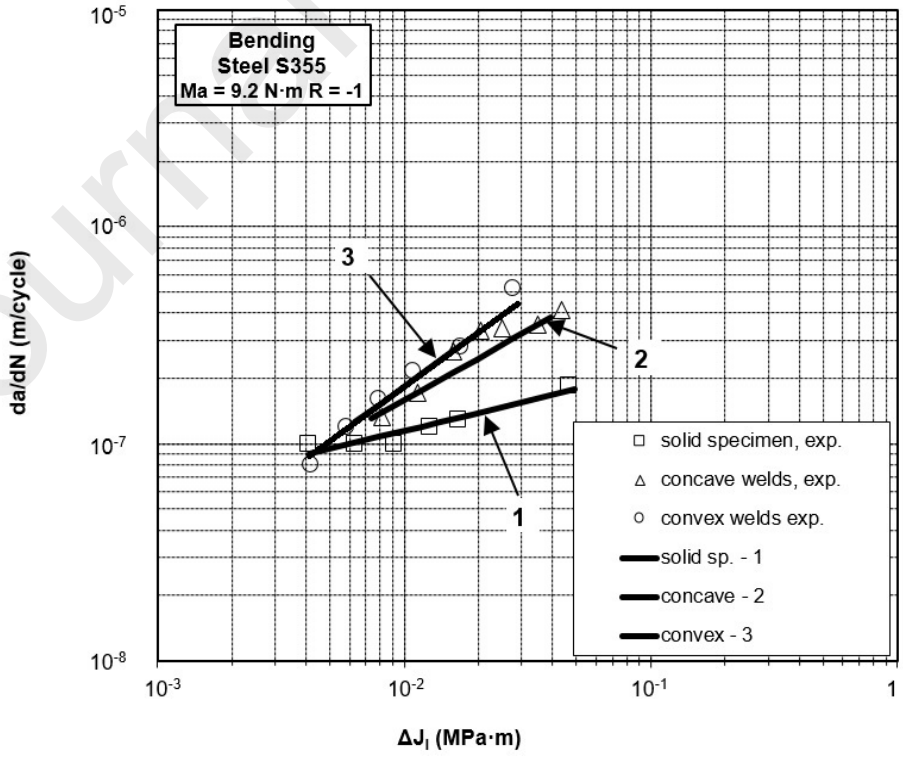

b)

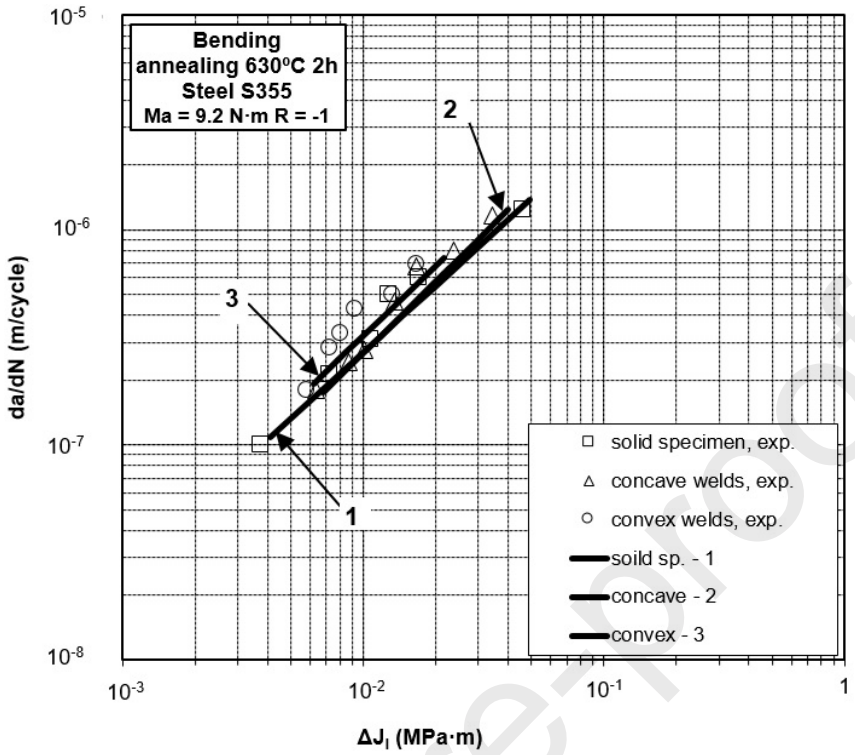

Figure 9

a)

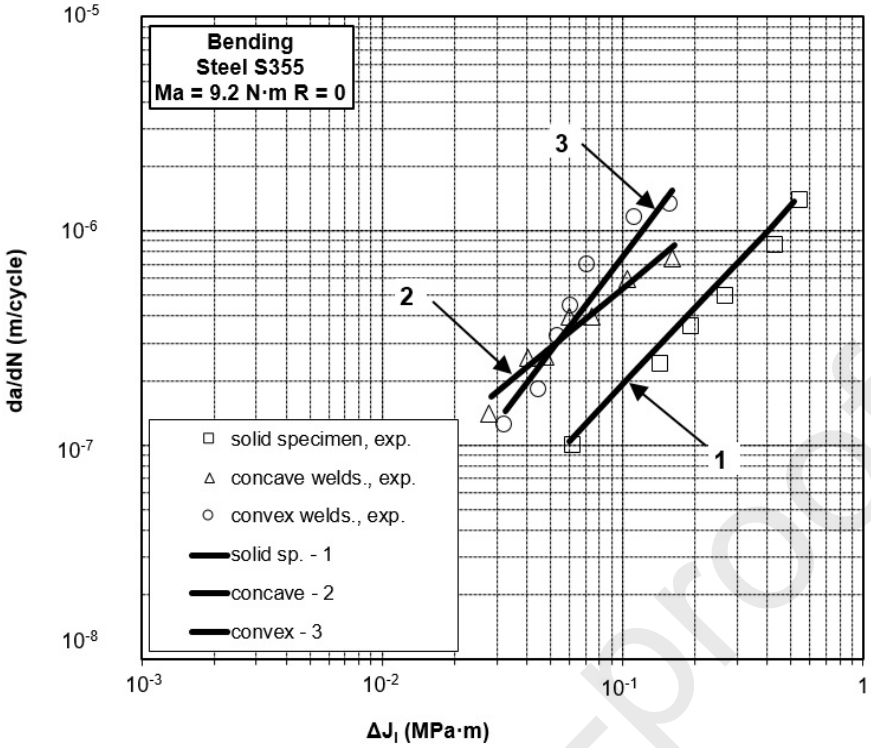

b)

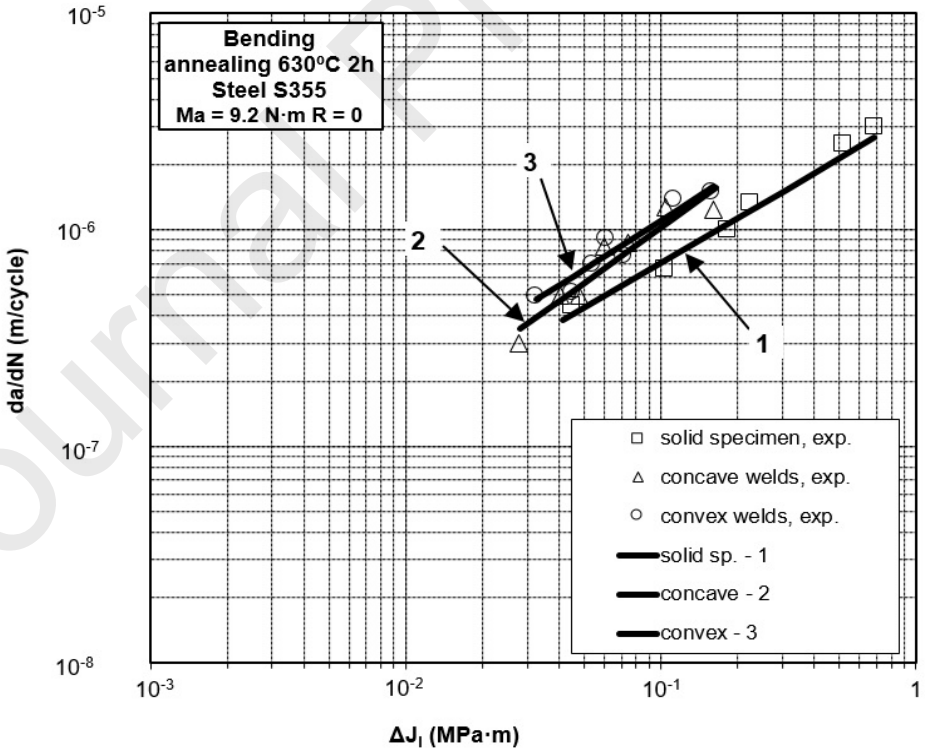

Figure 10

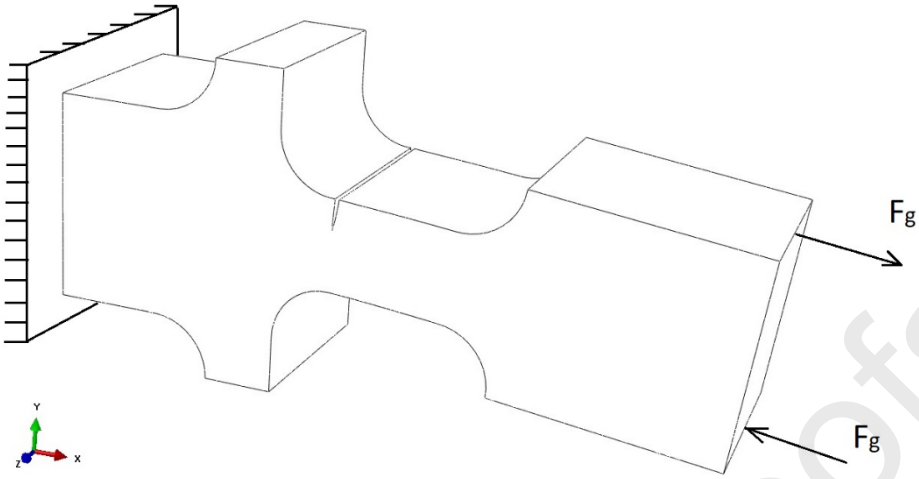

Figure 11

a)

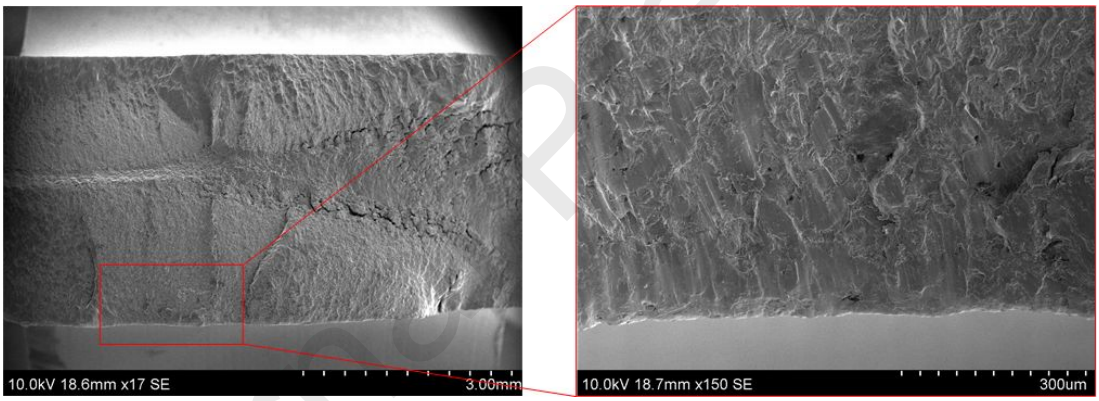

b)

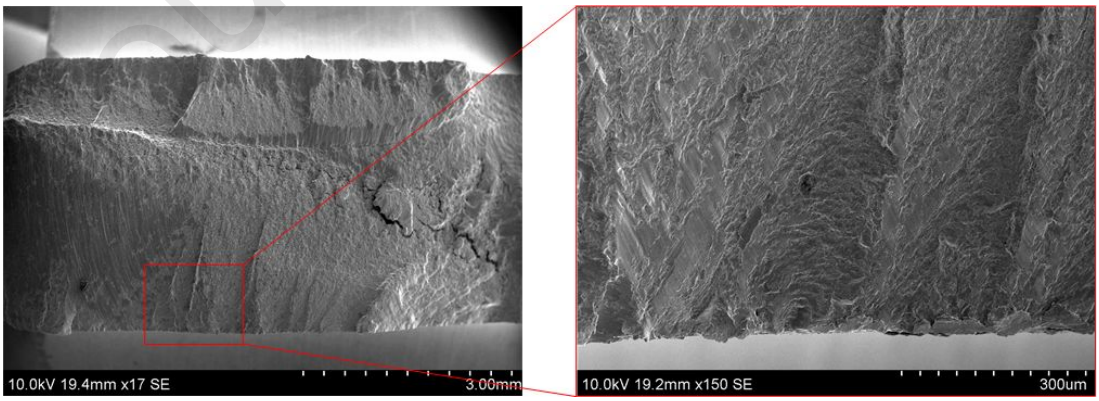

c)

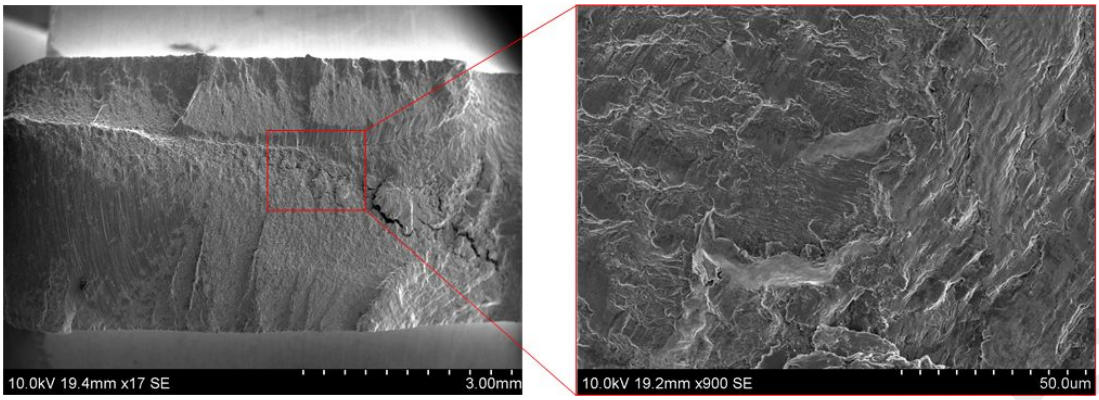

d)

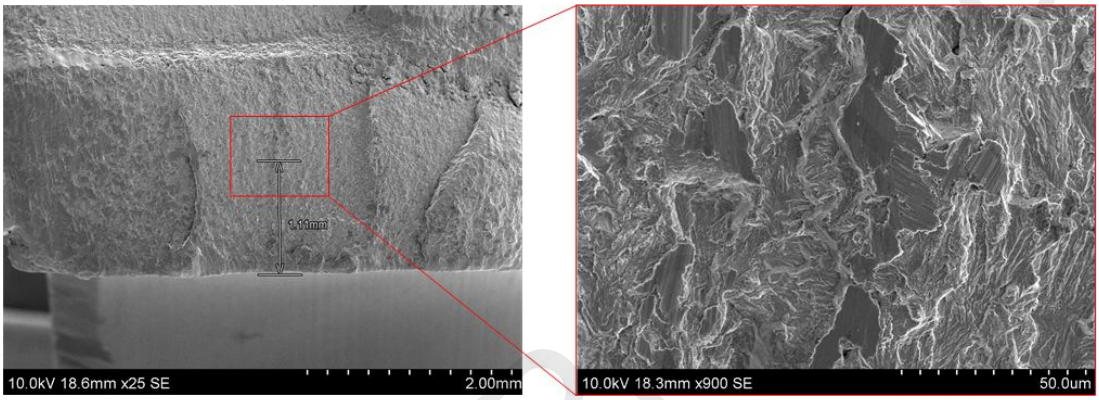

Table 1

C	Mn	Si	P	S	Cr	Ni	Cu	Fe
0.2	1.49	0.33	0.023	0.024	0.01	0.01	0.035	Bal.

Table 2

σ_y (MPa)	σ_u (MPa)	E (GPa)	ν	A_5 (%)
357	535	210	0.30	21

Table 3

Figure	graph	C, $m/(MPa \cdot m)^m$ cycle	m	r
8a	1	$4.037 \cdot 10^{-7}$	0.273	0.951
8a	2	$3.360 \cdot 10^{-7}$	0.574	0.872
8a	3	$8.179 \cdot 10^{-6}$	0.824	0.990
8b	1	$3.010 \cdot 10^{-5}$	1.023	0.999
8b	2	$4.412 \cdot 10^{-5}$	1.108	0.999
8b	3	$4.637 \cdot 10^{-5}$	1.078	0.998
9a	1	$2.999 \cdot 10^{-6}$	1.196	0.998
9a	2	$4.551 \cdot 10^{-6}$	0.925	0.999
9a	3	$2.262 \cdot 10^{-5}$	1.473	0.999
9b	1	$3.451 \cdot 10^{-6}$	0.691	0.993
9b	2	$7.196 \cdot 10^{-6}$	0.847	0.999
9b	3	$6.282 \cdot 10^{-6}$	0.753	0.999

Highlights

- The effect of HT and different R on the durability of the samples was explored.
- The effect of the energy approach on FCGR was explored.
- Description using the energy model showed better predictive than other approaches.
- The hardness in the HAZ and the joint is greater than that of the starting metal.

Declaration of Interest Statemen

We would like to confirm that all authors have seen and approved the final version of the manuscript being submitted. They warrant that the article is the authors' original work, hasn't received prior publication and isn't under consideration for publication elsewhere.

Sincerely yours
Dariusz Rozumek

Declaration of interests

☒ The authors declare that they have no known competing financial interests or personal relationships that could have appeared to influence the work reported in this paper.

☐The authors declare the following financial interests/personal relationships which may be considered as potential competing interests: